SIMULATION OF BIOMOLECULAR DIFFUSION AND COMPLEX FORMATION

STUART A. ALLISON,* SCOTT H. NORTHRUP,‡ AND J. ANDREW MCCAMMON§
Department of Chemistry, Georgia State University, Atlanta, Georgia 30303; ‡Department of Chemistry, Tennessee Technological University, Cookeville, Tennessee 38505; and §Department of Chemistry, University of Houston, Houston, Texas 77004

ABSTRACT Diffusion is a phenomenon of very widespread importance in molecular biophysics. Diffusion can determine the rates and character of the assembly of multisubunit structures, the binding of ligands to receptors, and the internal motions of molecules and assemblies that involve solvent surface displacements. Current computer simulation techniques provide much more detailed descriptions of diffusional processes than have been available in the past. Models can be constructed to include such realistic features as structural subunits at the submolecular level (domains, monomers, or atoms); detailed electrostatic charge distributions and corresponding solvent-screened inter- and intramolecular interactions; and hydrodynamic interactions. The trajectories can be analyzed either to provide direct information on biomolecular function (e.g., the bimolecular rate constant for formation of an electron-transfer complex between two proteins), or to provide or test models for the interpretation of experimental data (e.g., the time dependence of fluorescence depolarization for segments of DNA). Here, we first review the theory of diffusional simulations, with special emphasis on new techniques such as those for obtaining transport properties of flexible assemblies and rate constants of diffusion-controlled reactions. Then we survey a variety of recent applications, including studies of large-scale motion in DNA segments and substrate "steering" in enzyme-substrate binding. We conclude with a discussion of current work (e.g., formation of protein complexes) and possible areas for future work.

INTRODUCTION

The theoretical study of the motion of biological molecules is emerging as an important field of molecular biology. Two complementary techniques used to study these motions are molecular dynamics and Brownian dynamics. In molecular dynamics, a computer is used to solve the Newtonian equations of motion for the atoms in a system of interest for a finite period of time. The method has been applied to proteins, nucleic acids, and other biological molecules. These calculations have provided many fundamental new insights into the nature of biological molecules, as discussed in a number of reviews (1, 2).

One of the limitations of the standard molecular dynamics method is that only short time periods, usually less than a nanosecond, are accessible on present-day computers. The time ranges explored by relaxation techniques such as nuclear magnetic resonance (NMR), dynamic light scattering, and electric birefringence are much longer. Furthermore, most biological activity occurs over longer time periods. The rates of many biochemical processes depend on the frequency with which reaction partners encounter each other in solution (3–8). Examples of such "diffusion controlled" processes are known in the areas of enzyme-substrate catalysis, antibody-antigen binding, protein-DNA interaction, etc. (7). Diffusion is an intrinsically slow process. The time required for even a small molecule to diffuse 5 Å in water may exceed 500 ps. The technique of Brownian dynamics, which is based on diffusion or Langevin equations, can be used to simulate the long-time dynamical behavior of model systems (9).

In Brownian dynamics, a simplified model is used to represent the actual system, although the investigator has considerable freedom in its design. A series of increasingly realistic models of a particular system can be studied in a systematic way. A protein, for example, can be modeled as a single sphere derived from its hydrodynamic radius (10, 11), or as an array of spheres, each of which might correspond to a rigid domain or residue of the protein (12). Similarly, a DNA restriction fragment can be modeled as a stiff string of touching beads (13). One can include in a straightforward manner forces arising from electrostatic interactions between charged subunits; stretching, bending, and constraint forces in semirigid arrays of subunits; and other interactions. The solvent is represented as a viscous continuum that exerts stochastic forces on the model subunits. Solvent structural features (e.g., screening of Coulombic interactions by mobile ions) can be incorporated through appropriate potentials of mean force for the subunit interactions.

The Brownian dynamics method has two limitations relative to molecular dynamics. First, because solvent-averaged potentials are used, one cannot obtain detailed information on solvation structures (e.g., the pattern of

hydrogen bonds in water molecules around a solute). The average effects of such structures can, however, be incorporated into the potentials of mean force. Second, one cannot get information on the details of inertial motions that are evident during very short intervals of time, because the underlying diffusion equations describe the average motion of solutes whose motions have been interrupted by at least a few collisions with solvent molecules. Brownian dynamics gives a reliable description of solute motions for times longer than the solute momentum relaxation time (9); for typical biopolymer systems, this is <0.1 ps (12).

The most direct application of Brownian dynamics involves the determination of transport coefficients (diffusion constants) for rigid and semiflexible structures. Several numerical methods are available for determining transport coefficients of rigid structures modeled as arrays of spheres (14), but this is not the case for flexible structures. However, analytical techniques developed by a number of investigators are appropriate for certain classes of problems (15, 16). Transport properties for models of arbitrary complexity can be obtained from Brownian dynamics simulation. These are obtained either by carrying out a large number of single dynamics step "trajectories" starting from representative initial configurations followed by averaging the appropriate displacements (17), or by averaging over trajectories that are propagated for longer periods of time (13, 17–18).

In this discussion, we consider two examples of the application of Brownian dynamics to study internal or relative motions of biological molecules. In each case, the model system is allowed to evolve with time by taking successive dynamics steps to generate a trajectory (13). In the first example, relaxation "experiments" (fluorescence depolarization and depolarized light scattering) are simulated by appropriate averaging of a large number of trajectories. The system studied is a DNA restriction fragment modeled as a stiff string of touching beads. In the second example, the same basic procedure is used, but applied to bimolecular diffusion-controlled reactions. From a large number of Brownian dynamics trajectories, one obtains a recombination probability for two reactive species that start at some initial separation. This recombination probability can then be related directly to a rate constant (19). This method is applied to the diffusion-controlled enzyme-substrate reaction between superoxide dismutase and superoxide.

THEORY

Brownian dynamics is a method that allows one to simulate the diffusional motion of an assembly of interacting solute molecules. Consider first the simple case of an isolated spherical molecule in the absence of any direct force. If the particle were initially located at some point $\mathbf{R}^0$, then the probability density, $\rho(\mathbf{R}, \Delta t)$, of finding it at $\mathbf{R}$ after time Δt is given by

$$\rho(\mathbf{R}, \Delta t) = (4\pi D\Delta t)^{-3/2} \exp\left(-(\mathbf{R} - \mathbf{R}^0)^2/4D\Delta t\right), \quad (1)$$

where D is the translational diffusion constant of the molecule. In a simulation, the new position of the particle is selected at random from this Gaussian distribution. If a large number of steps using the same $\mathbf{R}^0$ and Δt for each were carried out, then the distribution of final positions must obey Eq. (1) above. The first step of the diffusional trajectory is then

$$\mathbf{R} = \mathbf{R}^0 + \mathbf{S}, \quad (2)$$

where $\mathbf{S}$ is a vector of Gaussian random numbers. The components of $\mathbf{S}$ have zero mean ($\langle S_\alpha \rangle = 0$; $\alpha = x$, y, or z) and have the variance

$$\langle S_\alpha S_\beta \rangle = 2D\delta_{\alpha\beta}\Delta t, \quad (3)$$

where $\delta_{\alpha\beta}$ is the Kronecker delta. $\delta_{\alpha\beta} = 1$ if $\alpha = \beta$ and equals 0 otherwise. Physically, $\mathbf{S}$ represents the stochastic displacement of the spherical molecule resulting from collisions with solvent. A trajectory can be extended to longer times ($2\Delta t$, $3\Delta t$, etc.) by repeated application of this algorithm with each step beginning at the position chosen in the previous step. By computing a large number of such trajectories with different random numbers, one generates a description of how an ensemble of diffusing molecules behaves.

When direct forces act on an isolated spherical particle (such as the centrifugal force on a sedimenting globular protein), it is necessary to account for the displacement that arises as a result of these forces. Eq. 2 is replaced with

$$\mathbf{R} = \mathbf{R}^0 + \mathbf{S} + \mathbf{F}^0\Delta t/f = \mathbf{R}^0 + \mathbf{S} + \frac{\Delta t}{k_B T} D\,\mathbf{F}^0, \quad (4)$$

where f is the friction constant, k_B is Boltzmann's constant, T is the absolute temperature, and $\mathbf{F}^0$ is the initial direct force on the molecule. A single dynamics step should be short enough so that $\mathbf{F}$ remains essentially constant as the molecule is displaced from $\mathbf{R}^0$ to $\mathbf{R}$ in time Δt.

When more than one spherical molecule or particle is present, they interact indirectly with each other by perturbing the velocity of the intervening solvent (hydrodynamic interaction) and perhaps directly through direct forces. A number of Brownian dynamics algorithms are available (9, 20–21), but in this work the algorithm of Ermak and McCammon is used (9). For a system of N interacting spherical subunits, the position of subunit i, $\mathbf{R}_i$, after a dynamics step of duration Δt, is given by

$$\mathbf{R}_i = \mathbf{R}_i^0 + \mathbf{S}_i + \frac{\Delta t}{k_B T}\sum_{j=1}^{N} \mathbf{D}_{ij}^0 \cdot \mathbf{F}_j^0, \quad (5)$$

where $\mathbf{R}_i^0$ is the initial position of subunit i. As in the single particle case, displacement results from direct forces ($\mathbf{F}$) and solvent collisions ($\mathbf{S}$). However, the diffusion constant of Eq. (4) is replaced by a generalized diffusion tensor, $\boldsymbol{D}$. These tensors represent the coupling of the motions of different subunits by hydrodynamic interaction (HI). As in the case of a single particle, the mean of the stochastic displacements is zero, but the generalized variance must satisfy the following condition

$$\langle \mathbf{S}_i \mathbf{S}_j \rangle = 2\,\boldsymbol{D}_{ij}\Delta t. \quad (6)$$

Methods of constructing $\mathbf{S}_i$ are described elsewhere (9, 20).

As a lowest-order approximation, HI between different subunits can be ignored completely. In this case $\boldsymbol{D}_{ij} = D_i\,\delta_{ij}\,\boldsymbol{I}$ where $\boldsymbol{I}$ is a 3×3 identity tensor and D_i is the translational diffusion constant of subunit i. For a relatively large, neutral sphere, the Stokes-Einstein equation gives

$$D_i = k_B T/6\,\pi\,\eta\,a_i, \quad (7)$$

where a_i is the radius of subunit i and η is the solvent viscosity. For small molecules (comparable to the size of the solvent molecules) (22) or molecules that interact strongly with the solvent (ions in water, for

example) (23), the observed diffusion constant may differ from the Stokes-Einstein value by a numerical factor that is usually in the range 0.5 to 2.0.

At the higher level, HI can be approximated using the Oseen (24) or Rotne-Prager (25) tensors. For identical nonoverlapping spheres of radius a, the latter tensor is given by

$$\mathbf{D}_{ij} = \frac{k_B T}{6\pi\eta a}\mathbf{I} = \mathrm{D}_0\,\mathbf{I} \qquad (i = j)$$

$$\mathbf{D}_{ij} = \frac{3aD_0}{4\mathrm{R}}\left[\left(\mathbf{I} + \frac{\mathbf{R}\,\mathbf{R}}{R^2}\right) + \frac{2a^2}{R^2}\left(\frac{1}{3}\mathbf{I} - \frac{\mathbf{R}\,\mathbf{R}}{R^2}\right)\right](\mathrm{i} \neq \mathrm{j}) \qquad (8)$$

where $R = |\mathbf{R}_i - \mathbf{R}_j|$. The Oseen tensor (stick boundary conditions) is obtained by omitting the a^2/R^2 terms on the right-hand side of Eq. 8. Other tensors (Oseen [26], Rotne-Prager for overlapping spheres [14, 25], as well as higher order [27]) are described elsewhere. For different subunits, it can be seen from Eq. 8 that $\boldsymbol{D}_{ij}$ falls off as a/R. If the subunits are far apart, HI is small.

Attention shall now be turned to the problem of obtaining a bimolecular rate constant for diffusion-controlled reactions by Brownian dynamics simulation. Smoluchowski and Debye investigated the problem of diffusion-controlled reactions between uniformly reactive spheres in the absence and presence of centrosymmetric Coulombic forces (4). More recently, there has been a proliferation of theoretical studies based on more refined models, as described in recent reviews (6–8). Perhaps the most advanced analytical-numerical methods are those based on the formalisms of Wilemski and Fixman (28), Keizer (29), and Zeintra et al. (30). The Brownian dynamics simulation method is sufficiently general to model systems of arbitrary configurational complexity and arbitrary inter- and intramolecular forces; and it allows for inclusion of hydrodynamic interaction. When a variety of interactions are present between the reactive species, there is probably little hope of obtaining analytical rate constants at a detailed level and recourse to simulation methods becomes necessary.

As an example, one can imagine generating diffusional trajectories of a substrate relative to an enzyme target. From the frequency of collisions of properly oriented substrates with the active site of the enzyme, a rate constant could then be calculated. In practice, this approach encounters the difficulty that many trajectories wander far from the enzyme. To determine the ultimate fate of such trajectories (whether they return and lead to reaction, or escape reaction altogether) would require infinitely long simulations. Recently, Northrup et al. have devised a method to circumvent this difficulty (19). The diffusion space around the enzyme is divided into two regions. The "inner" region is finite and comprises that volume adjacent to the enzyme in which the interactions are complicated and best dealt with numerically. The "outer" region is of infinite volume but is everywhere far enough from the enzyme so that the diffusional behavior can be described analytically. Trajectories then need be computed only in the finite inner regions. Let the target (enzyme) be surrounded by a spherical surface of radius b which lies just outside the inner region. Then the rate constant, k, can be written

$$k = k_D(b)\,p, \qquad (9)$$

where p is the probability that the reactant pair, starting at initial separation $r = b$, will ultimately react, and $k_D(b)$ is the steady-state rate at which reactants with separation $r > b$ first strike the b-surface. Because of the restrictions placed on b, $k_D(b)$ can be determined analytically (6)

$$k_D(b) = \left(\int_b^\infty dr\left[\frac{\exp[u(r)/k_B T]}{4\pi r^2 D(r)}\right]\right)^{-1}, \qquad (10)$$

where $u(r)$ is the (centrosymmetric) potential of mean force (i.e., the effective interaction energy between enzyme and substrate), and $D(r)$ is the relative diffusion constant. In the special case of no hydrodynamic interaction

$$D(r) = D_{rel} = D_1 + D_2, \qquad (11)$$

where D_1 and D_2 are the translational diffusion constants of the individual reactants.

To avoid the problem of reactants initially at $r = b$ diffusing to large distances, trajectories are terminated if r exceeds some cutoff distance $q > b$. What is actually determined in a simulation over many trajectories is a recombination probability, β, which is different from the desired p. This is because it is conceivable that a trajectory with $r > q$ would eventually react if it were not terminated at $r = q$. Fortunately, it is possible to correct β to obtain p using branching arguments; it can be shown that

$$p = \frac{\beta}{1 - (1 - \beta)k_D(b)/k_D(q)}. \qquad (12)$$

This point is discussed in more detail elsewhere (19).

RESULTS

Relaxation Experiments on DNA Restriction Fragments

The DNA molecule is modeled as a string of N touching beads of radius a linked end-to-end by $N - 1$ virtual bonds. Following Hagerman and Zimm (31), a bead radius of 15.9 Å was used because this yields a structure that mimics the overall hydrodynamic behavior of a continuous worm-like chain cylinder with radius 13 Å (corresponding to DNA). Bending forces were derived from the potential (32)

$$U_{bend} = \frac{g}{2}\sum_{j=1}^{N-2}\theta_j^2, \qquad (13)$$

where g is the bending force constant and θ_j is the angle between virtual bond vectors j and $j + 1$. The persistence length, P, is related to g by the expression (32)

$$g = Pk_B T/2a. \qquad (14)$$

In this work, P is varied from 200 to 800 Å and $N = 30$, corresponding to a fragment 922 Å long. Stretching forces that hold neighboring beads at a nearly constant separation of $2a$ are introduced using a displaced quadratic potential with a stiff force constant. This was found to yield results identical with earlier studies where fixed bond length constraints were used (13), but the present method is computationally more efficient. HI was included in the simulation using the Rotne-Prager tensor (Eq. 8), but these tensors were "preaveraged" to avoid the necessity of recomputing $\boldsymbol{D}_{ij}$ repetitively as the molecules deform during dynamics. In a comparative study of 10 subunit chains, it was found that "experiments" on preaveraged and nonpreaveraged chains were essentially identical.

To simulate fluorescence depolarization (fd), it is assumed that a dye molecule is rigidly attached to the structure. For the sake of illustration, the dye is placed near the center of the chain with its emission dipole colinear with a virtual bond vector. The polarization

anisotropy is then given by (13, 33)

$$r(t) = 0.4 \langle P_2[\mathbf{u}(t) \cdot \mathbf{u}(0)] \rangle$$
$$= 0.4 \exp [-3 \langle \theta^2(t) \rangle / 2], \quad (15)$$

where P_2 is a Legendre polynomial, $\mathbf{u}(t)$ is a unit vector along a particular bond of the chain at time t, and $\langle \theta^2(t) \rangle$ denotes the mean square angular displacement of that unit vector. This is the average that must be determined to simulate fd. For a rigid structure, $\langle \theta^2(t) \rangle = 4 \langle D_R \rangle t$ where brackets denote the average over a large number of structures and D_R is the rotational diffusion constant about an axis perpendicular to $\mathbf{u}$. For a flexible structure, $\langle \theta^2(t) \rangle$ is a complicated function of time. In depolarized light scattering, the relevant average is a reduced dynamic structure factor defined by (34)

$$g(t) = (N-1)^{-2} \sum_{i,j=1}^{N-1} \langle P_2[\mathbf{u}_i(t) \cdot \mathbf{u}_j(0)] \rangle, \quad (16)$$

where $\mathbf{u}_i(t)$ is the unit vector along the ith bond at time t. This is similar to the expression for $r(t)$, except that cross correlations between all virtual bonds, corresponding to different anisotropic scattering elements, are included in the average. In the special case of rigid structures, this reduces to

$$g(t) = g(0) \exp [-6 \langle D_r \rangle t], \quad (17)$$

which is identical to $r(t)$ except for a constant scaling factor. This is not the case, however, for flexible DNA fragments, as shown in Figs. 1 and 2 (note the different vertical scales). These two "experiments" were carried out using the same simulation of 280 trajectories selected at random from a Boltzmann distribution of starting configurations. Evidently, fd is more sensitive to rapid internal motions even though both experiments reveal flexibility on the time scale 0 to 200 ns. If the DNA fragments were behaving as rigid bodies, the dotted lines on Figs. 1 and 2 would have been observed corresponding to $\langle D_R \rangle = 2.5 \times 10^4$ s (31). The strong dependence of fd on flexibility is shown in Fig. 3. The stiffer the molecule, the lower the depolarization at both short and long times. The long-time behavior can be readily understood, because a stiff molecule has a larger average end-to-end distance and hence a smaller rotational diffusion constant (31). These results and others will be described more fully in a future publication.[1]

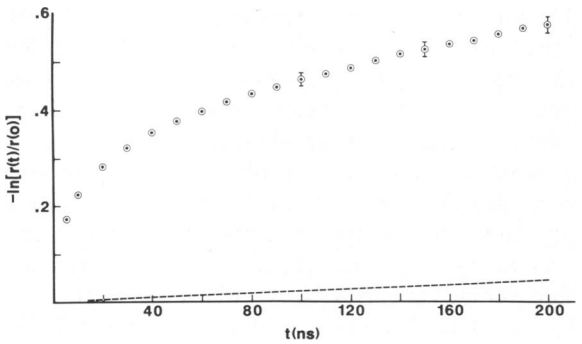

FIGURE 1 Fluorescence depolarization of a short wormlike chain: P = 400 Å, L = 922 Å. The transition moment lies along the local symmetry axis of the chain located near its center. The dotted line represents the behavior expected of an ensemble of rigid chains with the same P and L.

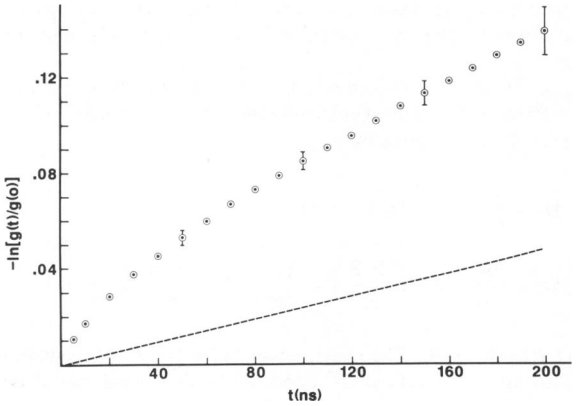

FIGURE 2 Depolarized light scattering (Eq. 16) of a short wormlike chain: P = 400 Å, L = 922 Å. Details in Fig. 1.

The error bars on selected data points were obtained from standard deviations of equivalent but independent subsimulations. For example, the 280 trajectories of Figs. 1 and 2 represent seven subsimulations of 40 trajectories each. These results required ~25 h of CPU time on a UNIVAC 1100 computer. However, we anticipate this could be reduced by a factor of 100 using a CYBER 205 supercomputer.

Diffusion-Controlled Reaction Between Superoxide and Superoxide Dismutase

Electrostatic interactions influence the rates of many biomolecular associations (4). For example, the charge distribution of a particular enzyme-substrate system may help to draw the two species together and "steer" them into a proper relative orientation for a catalytic reaction. Particularly interesting in this regard is the diffusion-controlled transformation of superoxide (O_2^-) catalyzed by the enzyme copper, zinc superoxide dismutase (SOD) (35, 36). The rate constant for this transformation has the unusual feature of decreasing with increasing salt concentration despite the fact that both species are negatively charged at neutral pH (37). It has been argued that these results are due to the noncentrosymmetric charge distribution of the dimeric enzyme (36).

In initial studies (10, 11), the SOD dimer and O_2^- were modeled as spheres with radii 28.5 and 1.5 Å. Two reactive

[1]Allison, S. A., "Brownian Dynamics Stimulation of Wormlike Chains, Fluorescence Depolarization and Depolarized Light Scattering," submitted to Macromolecules.

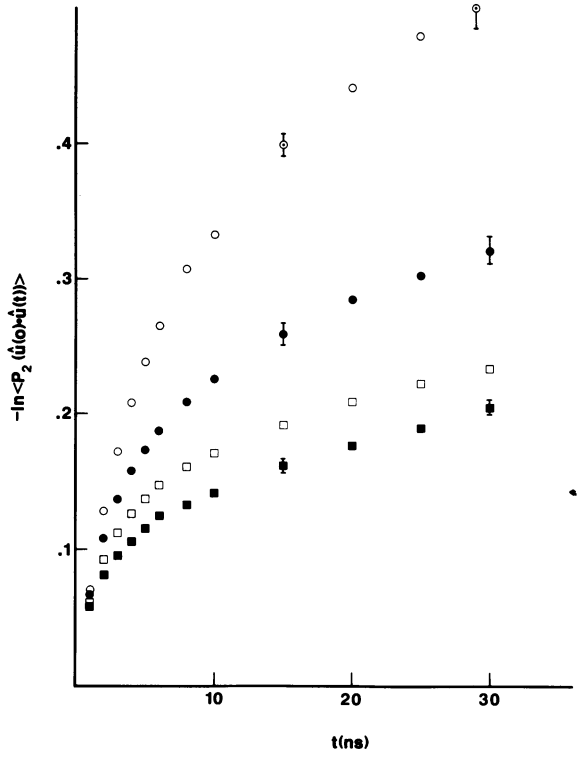

FIGURE 3 Effect of P on fluorescence depolarization from 30 subunit wormlike chains. **u** is a unit vector located at the chain center. P (Å) = 200 (○), 400 (●), 600 (□), 800 (■).

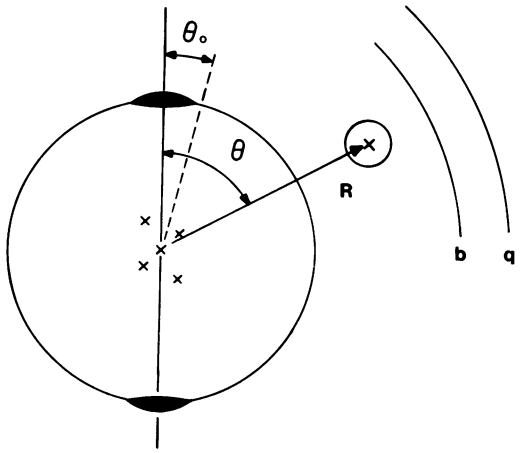

FIGURE 4 Schematic illustration of the superoxide dismutase O_2^- model. Crosses indicate positions of several charges. Active sites are indicated by the dark caps on the SOD sphere; $\theta_0 = 10°$.

patches corresponding to the active site regions of SOD were defined by surface points within 10° of an axis running through the center of the sphere (Fig. 4). Trajectories were usually initiated at b = 300 Å and terminated after collision with the active site or with a truncation sphere at q = 500 Å. A series of increasingly realistic electrostatic models was studied as summarized below.

(*A*) *One-Charge Model*: A single charge of −4 was placed at the center of the enzyme to represent the net charge.

(*B*) *Three-Charge Model*: Derived from Model C below by angular averaging the electrostatic potential about the axis passing through the center of the two reactive patches.

(*C*) *Five-Charge Model*: Designed to reproduce the monopole, dipole, and quadrupole moments associated with the charged groups in the x-ray structure of SOD (38).

(*D*) *76-Charge Model*: Charges were placed at the crystallographic coordinates of the 76-charged residues of SOD dimer.

(*E*) *2196-Charge Model*: Partial charges were assigned to all nonhydrogen atoms of the SOD dimer.

A dielectric constant of 78 was assumed throughout. Also, HI was ignored since it was previously found to have little effect on "steering" even though it does reduce the rate (39). Reduced rate constants are given in Table I ($X = k/k^0$, where $k^0 = 4\pi D_{rel}$ [30 Å]) for the different electrostatic models in the absence of added salt. Note that the rate for the single charge model is significantly lower than the other rates, which shows that the charge distribution of the enyzme does indeed steer superoxide toward the active site. Surprisingly, models *B* through *E* yield essentially the same rate. Although the charge distribution leads to a rate enhancement, it is the long range character of this distribution that affects the rate in the case of SOD.

Salt effects can be represented using simple Debye-Hückel type models for point or finite ions. Using model *C*, the reaction rate first increased, and then decreased to a plateau as the solvent ionic strength was increased (11). The initial behavior at low salt can be attributed to screening out repulsive net charge (monopole) interactions. At higher salt, where the shorter-ranged attractive forces are screened, this trend is reversed.

The initial studies are currently being extended in a number of ways. These include improvements in the dielectric model, more realistic treatment of solvent ions, and accounting more accurately for the surface topography of the enzyme. Generalizations of the original method (19) have also made it possible to initiate trajectories with the two reactive species in closer proximity (40).

TABLE I
REDUCED RATES FOR VARIOUS ELECTROSTATIC MODELS OF ZINC SUPEROXIDE DISMUTASE (SOD)

Model	No. of charges	X
A	1	0.056 ± 0.004
B	3	0.074 ± 0.004
C	5	0.079 ± 0.005
D	76	0.082 ± 0.011
E	2196	0.080 ± 0.006

CONCLUSION

Simulation methods are expected to open the way for detailed study of a wide variety of diffusional phenomena in cellular and molecular biology. The internal motions of flexible structures such as immunoglobulins or myosin as well as fluorescence energy transfer between donors and acceptors on the same or different molecules (as in a flexible polymer) could be studied by the methods described here. Studies of enzyme-substrate binding can be extended to predict the effects of amino acid sequence changes. Other refinements might include incorporation of internal flexibility of enzyme or substrate that would modulate the reactivity of active sites. The association of protein or protein-DNA complexes can be studied as a straightforward extension of the work on SOD. Other simple association phenomena (e.g., antigen-antibody, hormone-receptor) can be handled in the same way. The increasing availability of supercomputers will make substantially more sophisticated modeling possible in the future.

S. A. Allison is the recipient of a Presidential Young Investigator Award, a Camille and Henry Dreyfus Grant for Newly Appointed Faculty in Chemistry, and a grant from the Research Corporation. S. H. Northrup is the recipient of a National Institutes of Health (NIH) Research Career Development Award (AM01403) and a grant from the Petroleum Research Fund. J. A. McCammon is an Alfred P. Sloan Research Fellow and is the recipient of an NIH Research Career Development Award (HL00664) and a Camille and Henry Dreyfus Teacher-Scholar Award. The research described here was supported in part by grants to the University of Houston from NIH (GM31749); the National Science Foundation (PCM8201204, PCM8404219); and the Robert A. Welch Foundation.

Received for publication 22 April 1985 and in revised form 31 May 1985.

REFERENCES

1. McCammon, J. A. 1984. Protein dynamics. *Rep. Prog. Phys.* 47:1–46.
2. Karplus, M., and J. A. McCammon. 1983. Dynamics of proteins: elements and function. *Annu. Rev. Biochem.* 52:263–300.
3. Knowles, J., and W. Alberty. 1977. Perfection of enzyme catalysis: the energetics of triosephosphate isomerase. *Acc. Chem. Res.* 10:105–111.
4. Neumann, E. 1981. *In* Structural and Functional Aspects of Enzyme Catalysis. H. Eggerer and R. Huber, editors. Springer-Verlag, Berlin. 45–58.
5. Chou, K., and G. Zhou. 1982. Role of protein outside active site on the diffusion-controlled reaction of enzyme. *J. Am. Chem. Soc.* 104:1409–1413.
6. Calef, D., and J. Deutch. 1983. Diffusion-controlled reactions. *Annu. Rev. Phys. Chem.* 34:493–524.
7. Berg, O., and P. von Hippel. 1985. Diffusion-controlled macromolecular interactions. *Annu. Rev. Biophys. Chem.* 14:131–160.
8. McCammon, J. A., S. H. Northrup, and S. Allison. 1985. Diffusional dynamics of ligand-receptor association. *Commun. Mol. Cell. Biophys.* In press.
9. Ermak, D., and J. A. McCammon. 1978. Brownian dynamics with hydrodynamic interactions. *J. Chem. Phys.* 69:1352–1360.
10. Allison, S., G. Ganti, and J. A. McCammon. 1985. Simulation of the diffusion-controlled reaction between superoxide and superoxide dismutase. I. simple models. *Biopolymers.* In press.
11. Allison, S., and J. A. McCammon. 1985. Dynamics of substrate binding to copper, zinc superoxide dismutase. *J. Phys. Chem.* 89:1072–1074.
12. McCammon, J. A., S. H. Northrup, M. Karplus, and R. Levy. 1980. Helix-coil transitions in a simple polypeptide model. *Biopolymers.* 19:2033–2045.
13. Allison, S., and J. A. McCammon. 1984. Multistep Brownian dynamics: application to short wormlike chains. *Biopolymers.* 23:363–375.
14. Garcia de la Torre, J., and V. Bloomfield. 1981. Hydrodynamic properties of complex, rigid, biological macromolecules: theory and application. *Quart. Rev. Biophys.* 14:81–139.
15. Wegener, W., 1982. Bead models of segmentally flexible macromolecules. *J. Chem. Phys.* 76:6425–6430.
16. Harvey, S., P. Mellado, and J. Garcia de la Torre. 1983. Hydrodynamic resistance and diffusion coefficients of segmentally flexible macromolecules with two subunits. *J. Chem. Phys.* 78:2081–2090.
17. Allison, S., and J. A. McCammon. 1984. Transport properties of rigid and flexible macromolecules by Brownian dynamics simulation. *Biopolymers.* 23:167–187.
18. Lee, S., and M. Karplus. 1985. Brownian dynamics simulations: statistical error of correlation functions. *J. Chem. Phys.* 81:6106–6118.
19. Northrup, S., S. Allison, and J. A. McCammon. 1984. Brownian dynamics simulation of diffusion influenced bimolecular reactions. *J. Chem. Phys.* 80:1517–1524.
20. Fixman, M. 1981. Inclusion of hydrodynamic interaction in polymer dynamical simulations. *Macromolecules.* 14:1710–1717.
21. Lamm, G., and K. Schulten. 1983. Extended Brownian dynamics II. reactive, nonlinear diffusion. *J. Chem. Phys.* 78:2713–2734.
22. Hynes, J. 1977. Statistical mechanics of molecular motion in dense fluids. *Annu. Rev. Phys. Chem.* 28:301–321.
23. Wolynes, P. 1980. Dynamics of electrolyte solutions. *Annu. Rev. Phys. Chem.* 31:345–376.
24. Oseen, C. 1927. *In* Mathematik und ihre Anwendaungen in Monographien und Lehrbüchern. E. Hilb, editor. Akademische Verlagsgesellschaft, Leipzig. Vol. 1.
25. Rotne, J., and S. Prager. 1969. Variational treatment of hydrodynamic interaction in polymers. *J. Chem. Phys.* 50:4831–4837.
26. Pear, M., and J. A. McCammon. 1981. Hydrodynamic interaction effects on local motions in chain molecules. *J. Chem. Phys.* 74:6922–6925.
27. Mazur, P., and W. van Saarloos. 1982. Many-sphere hydrodynamic interactions and mobilities in a suspension. *Physica.* 115*A*:21–57.
28. Wilemski, G., and M. Fixman. 1973. General theory of diffusion-controlled reactions. *J. Chem. Phys. 58:4009–4019.*
29. Keizer, J., 1981. Effect of diffusion on reaction rates in solution and in membranes. *J. Phys. Chem. 85:940–941.*
30. Zientra, G., J. Nagy, and J. Freed. 1980. Diffusion-controlled kinetics of protein domain coalescence: effect of orientation, interdomain forces and hydration. *J. Chem. Phys.* 73:5092–5106.
31. Hagerman, P., and B. Zimm. 1981. Monte Carlo approach to the analysis of the rotational diffusion of wormlike chains. *Biopolymers.* 20:1481–1502.
32. Schellman, J. 1974. Flexibility of DNA. *Biopolymers.* 13:217–226.
33. Schurr, J. M. 1984. Rotational diffusion of deformable macromolecules with mean local cylindrical symmetry. *J. Chem. Phys.* 84:71–96.
34. Carpenter, D., and J. Skolnick. 1981. Depolarized light scattering from macromolecules: effects of torsional oscillations, conformational transitions, and overall rotations. *Macromolecules.* 14:1284–1290.
35. Cudd, A., and I. Fridovich. 1982. Electrostatic interactions in the

reaction mechanism of bovine erythrocyte superoxide dismutase. *J. Biol. Chem.* 257:11443–11447.
36. Getzoff, E., J. Tainer, P. Weiner, P. Kollman, J. Richardson, and D. Richardson. 1983. Electrostatic recognition between superoxide and copper, zinc superoxide dismutase. *Nature (Lond.)*. 306:287–290.
37. Salin, M., and W. Wilson. 1981. Porcine superoxide dismutase. *Mol. Cell. Biochem.* 36:157–161.
38. Tainer, J., E. Getzoff, K. Beem, J. Richardson, and D. Richardson. 1982. Determination and analysis of the 2 Å structure of copper, zinc superoxide dismutase. *J. Mol. Biol.* 160:181–217.
39. Allison, S., N. Srinivasan, J. A. McCammon, and S. Northrup. 1984. Diffusion-controlled reactions between a spherical target and dumbell dimer by Brownian dynamics simulation. *J. Phys. Chem.* 88:6152-6157.
40. Allison, S., S. Northrup, and J. A. McCammon. 1986. Extended Brownian dynamics of diffusion controlled reactions. *J. Chem. Phys.* In press.

DISCUSSION

Session chairman: Adrian Parsegian
Scribes: Gary A. Griess and Eric T. Baldwin

BLOOMFIELD: The general technique of Brownian dynamic simulation is an attractive procedure that gets into the range of times where we do most of our experiments. What does diffusional simulation leave out (that molecular dynamics would include if it could be carried out), that would be important for analysis of experiments on the nanosecond and longer time scale? Also, can you estimate a lower bound to the time scale of Brownian dynamics? Does leaving out the velocity make a difference?

ALLISON: I think you can get to all times by overlapping molecular dynamics and Brownian dynamics. For example, molecular dynamics can get out to a couple hundred picoseconds. Brownian dynamics is applicable on time scales longer than the momentum relaxation times of the solvent, and this is on the order of a few tenths of a picosecond. Hence the two methods overlap. As for what is left out, Brownian dynamics replaces the solvent with a bath of random noise. The potentials are not real potentials but potentials of mean force. So you lose the detailed atomic description of the solvent when you go to Brownian dynamics.

BLOOMFIELD: What is your sense of the consequences of that particular omission for the valid analysis of physical situations?

ALLISON: When you ignore momentum relaxation but correct for it using random numbers to represent stochastic displacements, you must remember that the dynamics are being generated in a statistical rather than deterministic sense.

BLOOMFIELD: Macromolecular interactions depend strongly on water structure and its adjustment to the polymer's approach. Do you see any way of incorporating solvent into Brownian dynamics? What might its neglect leave out? The effective dielectric constant for electrostatic interactions is a related problem.

ALLISON: In Brownian dynamics, simulation of the diffusion-controlled reaction between the enzyme and the substrate the dielectric constant was set at 78, and this would certainly not be true if you were looking at the effective dielectric constant between two groups inside a protein. However, in this case, over much of the diffusional process the enzyme and substrate are separated by a fairly thick layer of water. To assume a bulk dielectric constant of water would be fairly accurate when enzyme and substrate are far apart. Presently, the Warwicker-Watson model, where you model the protein as one dielectric and the water as another dielectric, is being used to develop a more realistic model for this problem. This work is just getting under way, and we have no results yet. Our philosophy is to start with the simplest model and develop more and more sophisticated models. If the simple model works, that model should be used.

EISENBERG: In regard to the flexible DNA worm-like chain, I would like to know whether you can interpret some experiments which are well established (Kam, Borochov, and Eisenberg. 1981. *Biopolymers*. 20:2671–2690). The apparent diffusion constant, D_{app}, from quasielastic light scattering, yields the translational diffusion constant at low values of the scattering vector **q**, but increases in sigmoidal fashion with increasing values of **q**. If you stiffen up the molecule, can you see changes in the predicted relaxation times?

ALLISON: Yes, you can carry out the simulations over both high and low scattering vectors. Different experiments correspond to different averages over the internal coordinates of the worm-like chain. You would have to carry out the average over the appropriate physical quantity. I have done that for the 30 subunit worm-like chains, but the results are not particularly interesting. Polarized light scattering is not very sensitive to internal motions of 30 subunit worm-like chains unless the scattering vector is very large. You get a diffusion constant corresponding to that of the overall molecule. Different relaxation times depend on chain conformation and not on internal bending.

POTSCHKA: In macromolecules the location of the target of a reaction-diffusion process is usually quite different from the center of the molecule. Compared to the properties of the target the remainder of the molecule most often has only second-order influence via rotational diffusion. You interpret differences between a simple charge vs. five charge centers by the importance of multipole moments. Intuitively this should be a matter of radial distance away from the reaction center. Wouldn't a simpler model centered in the target do equally well?

ALLISON: The model of SOD enzyme has two active patches. If you put a charge at the center you have a charge monopole model. The five-charge model has charges pulled back inside the enzyme. Now, if you keep the quadrupole moment constant and move quadrupolar charges farther out ($\mathbf{q}a^2$ = constant, where **q** is the quadrupole charge and a the charge separation) the electrostatic potential doesn't change appreciably, as long as the quadrupolar charges are kept within the protein interior.

LEE: I would like to elaborate on Victor Bloomfield's question. Adrian Parsegian, Donald Rau, and I have measured a hydration force that